S©MR

СИБИРСКИЕ ЭЛЕКТРОННЫЕ
МАТЕМАТИЧЕСКИЕ ИЗВЕСТИЯ
Siberian Electronic Mathematical Reports
http://semr.math.nsc.ru
ISSN 1813-3304

Vol. 21, No. 2, pp. 144–145 (2024) УДК 519.67
https://doi.org/10.33048/semi.2024.21.??? MSC 15B33

A NEW COLOR IMAGE WATERMARKING SCHEME BASED ON SCHUR DECOMPOSITION OF COMMUTATIVE QUATERNION MATRICES

D. ZHANG

Communicated by P.P. Petrov

Abstract: To protect the copyright of color digital images in the current internet environment, we propose a color image watermarking scheme based on nonsubsampled contourlet transform (NSCT) and Schur decomposition of commutative quaternion matrices (SchurCQ), taking into account the correlation and synchronization issues between color channels. During the watermark embedding phase, the NSCT is employed to obtain the low-frequency component of the host image, which is then divided into non-overlapping 4×4 blocks. The SchurCQ decomposition is utilized to perform associated transformations across multiple color channels. Watermark information, encrypted by Arnold scrambling, is embedded into the largest diagonal element of the matrix through quantization index modulation. In the extraction phase, the watermark can be successfully retrieved from the attacked watermarked image without any reference to the original

---

Zhang D., A new color image watermarking scheme based on Schur decomposition of commutative quaternion matrices.

The article was prepared within the framework of the project "Mirror Laboratories" of HSE University and North-Eastern Federal University "Quaternions, geometric algebras and applications" (sections 2,3,4). The article is supported by the Ministry of Science and Higher Education of the Russian Federation, agreement No. FSRG-2023-0025 (sections 5,6).

Received January, 1, 2023, Published December, 31, 2023.

information. Numerical experiments show that the proposed scheme significantly enhances security and robustness while maintaining imperceptibility compared with other schemes.

Keywords: commutative quaternion matrix, Schur decomposition, contourlet transform, color image watermarking.

1 Introduction

Color image watermarking, by embedding secret information into multimedia content, has emerged as an effective technique for protecting digital media intellectual property from illegal operations, ensuring both copyright and content integrity and has become a hot research topic nowadays [1]. Depending on the application scenario, watermarks can be categorized into robust and fragile watermarks. Robust watermarks are primarily used to protect the ownership of digital media, while fragile watermarks serve to verify the integrity of images [2]. Furthermore, based on the information required for watermark extraction, watermarking schemes are divided into non(semi-)blind and blind schemes, where non(semi-)blind schemes require the host image and/or the original watermark, whereas blind schemes do not.

Existing color image watermarking schemes can be broadly classified into single-channel processing, multi-channel synthesis, and quaternion-based methods [3, 4]. Single-channel processing and multi-channel synthesis fundamentally deal with grayscale images, which may not fully capture the interrelationships between different color channels. In contrast, quaternion-based methods treat a color image as a purely imaginary quaternion matrix, enabling holistic processing of the color image without losing color information. As a special type of quaternion, commutative quaternions satisfy the commutative property of multiplication, reducing computational complexity while also preserving the color information in the holistic processing of color images [5]. Therefore, studying color image watermarking using quaternions or commutative quaternions has significant theoretical and practical implications. As more researchers recognize the importance of quaternions and commutative quaternions [6, 7, 8, 9, 10, 11], many have begun using them to explore color image watermarking.

In the paper [12], the authors proposed a color image watermarking scheme based on the quaternion Fourier transform. In the paper [13], the authors introduced a color image watermarking scheme based on quaternion QR decomposition (QQRD) by modifying the Q matrix in QQRD. In the paper [14], the authors proposed a color image watermarking scheme based on quaternion matrix singular value decomposition (SVDQ) by modifying the three smallest singular values of the quaternion matrix. Similarly, in the paper [15], the authors developed a color image watermarking scheme based on the commutative quaternion matrix SVD (SVDCQ) by changing the singular values of the commutative quaternion matrix. In some recent research, Schur decomposition has been applied to watermarking due to its lower computational complexity compared to other transformations such as SVD, showing potential to be a competitive alternative in the transform domain [16, 17, 18].

To ensure the efficiency and security of the watermarking scheme, this paper proposes a color image watermarking scheme based on the Schur decomposition of commutative quaternion matrices (SchurCQ), which combines commutative quaternion matrices, nonsubsampled contourlet transform (NSCT), and Arnold scrambling. The objective is to achieve high fidelity in the watermarked image and high quality in the extracted watermark. The specific advantages of the proposed scheme are as follows: (1) Novel algorithm: This is the first introduction of the Schur decomposition theorem and algorithm of commutative quaternion matrices. (2) Efficient scheme: The computational complexity of commutative quaternions is lower than that of quaternions, making the color image watermarking scheme based on SchurCQ and NSCT more efficient and less perceptible.

2 Preliminaries

For any commutative quaternions in [19] are defined as follows

$$q = q_1 + q_2\mathrm{i} + q_3\mathrm{j} + q_4\mathrm{k} \in \mathbf{H}_\mathrm{c}, \mathrm{j}^2 = 1, \mathrm{i}^2 = \mathrm{k}^2 = \mathrm{ijk} = -1, \tag{1}$$

where $q_1, q_2, q_3, q_4 \in \mathbf{R}, \mathrm{ij} = \mathrm{ji} = \mathrm{k}, \mathrm{jk} = \mathrm{kj} = \mathrm{i}, \mathrm{ki} = \mathrm{ik} = -\mathrm{j}$.

For any matrix $A = A_1 + A_2\mathrm{j} \in \mathbf{H}_\mathrm{c}^{m\times n}, A^T = \mathrm{Re}\,(A_1)^T + \mathrm{Im}\,(A_1)^T\,\mathrm{i} + \mathrm{Re}\,(A_2)^T\,\mathrm{j} + \mathrm{Im}\,(A_2)^T\,\mathrm{k}, \bar{A} = \mathrm{Re}\,(A_1) - \mathrm{Im}\,(A_1)\,\mathrm{i} - \mathrm{Re}\,(A_2)\,\mathrm{j} - \mathrm{Im}\,(A_2)\,\mathrm{k}, A^* = \mathrm{Re}\,(A_1)^T - \mathrm{Im}\,(A_1)^T\,\mathrm{i} - \mathrm{Re}\,(A_2)^T\,\mathrm{j} - \mathrm{Im}\,(A_2)^T\,\mathrm{k}, \widetilde{A} = \mathrm{Re}\,(A_1) - \mathrm{Im}\,(A_1)\,\mathrm{i} + \mathrm{Re}\,(A_2)\,\mathrm{j} - \mathrm{Im}\,(A_2)\,\mathrm{k}, A^H = \mathrm{Re}\,(A_1)^T - \mathrm{Im}\,(A_1)^T\,\mathrm{i} + \mathrm{Re}\,(A_2)^T\,\mathrm{j} - \mathrm{Im}\,(A_2)^T\,\mathrm{k}$, denote the transpose, the conjugate, the conjugate transpose, the ik-conjugate and the ik-conjugate transpose of the matrix A, respectively, where $A_1, A_2 \in \mathbf{C}^{m\times n}, \mathrm{Re}\,(A_1)$ is defined as real part of A_1, and $\mathrm{Im}\,(A_1)$ is defined as the imaginary part of A_1. Its complex representation A^σ was denoted by

$$A^\sigma = \begin{bmatrix} A_1 & A_2 \\ A_2 & A_1 \end{bmatrix} \in \mathbf{C}^{2m\times 2n}. \tag{2}$$

For any matrix $A \in \mathbf{H}_\mathrm{c}^{m\times n}$, we can obtain $(A^*)^\sigma \neq (A^\sigma)^*$ in general. But for the ik-conjugate transpose A^H of A, we have

$$\left(A^H\right)^\sigma = (A^\sigma)^H. \tag{3}$$

For $A, B \in \mathbf{H}_\mathrm{c}^{m\times n}$, $C \in \mathbf{H}_\mathrm{c}^{n\times s}$,$r \in \mathbf{R}$, we can get

$$(A + B)^\sigma = A^\sigma + B^\sigma, (AC)^\sigma = A^\sigma C^\sigma, (rA)^\sigma = rA^\sigma. \tag{4}$$

Clearly for $A = A_1 + A_2\mathrm{j} \in \mathbf{H}_\mathrm{c}^{m\times n}$, we have

$$P_m^T A^\sigma P_n = \begin{bmatrix} A_1 - A_2 & 0 \\ 0 & A_1 + A_2 \end{bmatrix}, \tag{5}$$

where $P_t = \frac{1}{\sqrt{2}}\begin{bmatrix} I_t & I_t \\ -I_t & I_t \end{bmatrix}, P_t^T P_t = P_t P_t^T = I_{2t}$.

Two norms of a matrix $A \in \mathbf{H}_c^{m\times n}$ are defined

$$\|A\|_F \equiv \frac{1}{\sqrt{2}}\|A^\sigma\|_F, \|A\|_2 \equiv \|A^\sigma\|_2, \tag{6}$$

then $\|\cdot\|_F$ and $\|\cdot\|_2$ are two unitarily invariant norms of commutative quaternion matrices.

3 Schur decomposition and generalized Schur decomposition of commutative quaternion matrices

Lemma 1. (Schur)[18, 20]. *Let $A \in \mathbf{F}^{m\times m}$, $\mathbf{F} = \{\mathbf{R}, \mathbf{C}, \mathbf{H}\}$. Then the Schur decomposition of the matrix A is as follows*

$$A = UDU^H, \tag{7}$$

where $U \in \mathbf{F}^{m\times m}$ is a unitary matrix, $D \in \mathbf{F}^{m\times m}$ is an upper triangular matrix that has the eigenvalues on the diagonal.

Now we study the Schur decomposition problem of commutative quaternion matrices. Let $A = A_1 + A_2\mathrm{j} \in \mathbf{H}_c^{m\times n}$, by (2), (5) and Lemma 1 there exist two unitary matrices $\hat{U}_1, \hat{U}_2 \in \mathbf{C}^{m\times m}$ and two upper triangular matrices $\hat{D}_1, \hat{D}_2 \in \mathbf{C}^{m\times m}$ such that

$$A_1 - A_2 = \hat{U}_1\hat{D}_1\hat{U}_1^H, \ A_1 + A_2 = \hat{U}_2\hat{D}_2\hat{U}_2^H. \tag{8}$$

By (5) and (8), we have

$$\begin{aligned}
A^\sigma =& P_m \begin{bmatrix} A_1 - A_2 & 0 \\ 0 & A_1 + A_2 \end{bmatrix} P_n^T \\
=& P_m \begin{bmatrix} \hat{U}_1 & 0 \\ 0 & \hat{U}_2 \end{bmatrix} \begin{bmatrix} \hat{D}_1 & 0 \\ 0 & \hat{D}_2 \end{bmatrix} \begin{bmatrix} \hat{U}_1^H & 0 \\ 0 & \hat{U}_2^H \end{bmatrix} P_m^T \\
=& P_m \begin{bmatrix} \hat{U}_1 & 0 \\ 0 & \hat{U}_2 \end{bmatrix} P_m^T P_m \begin{bmatrix} \hat{D}_1 & 0 \\ 0 & \hat{D}_2 \end{bmatrix} P_m^T P_m \begin{bmatrix} \hat{U}_1^H & 0 \\ 0 & \hat{U}_2^H \end{bmatrix} P_m^T \\
=& \begin{bmatrix} \frac{\hat{U}_1+\hat{U}_2}{2} & \frac{\hat{U}_2-\hat{U}_1}{2} \\ \frac{\hat{U}_2-\hat{U}_1}{2} & \frac{\hat{U}_1+\hat{U}_2}{2} \end{bmatrix} \begin{bmatrix} \frac{\hat{D}_1+\hat{D}_2}{2} & \frac{\hat{D}_2-\hat{D}_1}{2} \\ \frac{\hat{D}_2-\hat{D}_1}{2} & \frac{\hat{D}_1+\hat{D}_2}{2} \end{bmatrix} \begin{bmatrix} \frac{\hat{U}_1^H+\hat{U}_2^H}{2} & \frac{\hat{U}_2^H-\hat{U}_1^H}{2} \\ \frac{\hat{U}_2^H-\hat{U}_1^H}{2} & \frac{\hat{U}_1^H+\hat{U}_2^H}{2} \end{bmatrix} \\
=& (\frac{\hat{U}_1+\hat{U}_2}{2} + \frac{\hat{U}_2-\hat{U}_1}{2}\mathrm{j})^\sigma (\frac{\hat{D}_1+\hat{D}_2}{2} + \frac{\hat{D}_2-\hat{D}_1}{2}\mathrm{j})^\sigma (\frac{\hat{U}_1^H+\hat{U}_2^H}{2} + \frac{\hat{U}_2^H-\hat{U}_1^H}{2}\mathrm{j})^\sigma \\
=& U^\sigma D^\sigma (U^H)^\sigma,
\end{aligned} \tag{9}$$

where

$$U = \frac{\hat{U}_1+\hat{U}_2}{2} + \frac{\hat{U}_2-\hat{U}_1}{2}\mathrm{j}, \ D = \frac{\hat{D}_1+\hat{D}_2}{2} + \frac{\hat{D}_2-\hat{D}_1}{2}\mathrm{j}. \tag{10}$$

Clearly, U is a commutative quaternion unitary matrix, D is a commutative quaternion upper triangular matrix. Therefore, there exist a commutative quaternion unitary matrix U and a commutative quaternion upper triangular matrix D such that

$$A = UDU^H, \tag{11}$$

where $U \in \mathbf{H}_c^{m\times m}, U^H U = UU^H = I_m$.

Theorem 1. (SchurCQ). *Let $A \in \mathbf{H}_c^{m\times m}$. Then there exist a commutative quaternion unitary matrix U and a commutative quaternion upper triangular matrix $D \in \mathbf{H}_c^{m\times m}$ such that*

$$A = UDU^H, \tag{12}$$

where $U \in \mathbf{H}_c^{m\times m}, U^H U = UU^H = I_m$.

According to the Theorem 1, we also have the following algorithm for computing the Schur decomposition of commutative quaternion matrices.

Algorithm 1. (An algorithm for computing SchurCQ): For any commutative quaternion $A \in \mathbf{H}_c^{m\times m}$. Input A, output $U \in \mathbf{H}_c^{m\times m}$, $D \in \mathbf{H}_c^{m\times m}$, such that $A = UDU^H$.

Step 1. Find the matrix A^σ by (2);

Step 2. Find the following equation by (5),

$$P_m^T A^\sigma P_n = \begin{bmatrix} A_1 - A_2 & 0 \\ 0 & A_1 + A_2 \end{bmatrix};$$

Step 3. Construct Schur decomposition of $B_1 - B_2$ and $B_1 + B_2$, respectively,

$$B_1 - B_2 = \hat{U}_1 \hat{D}_1 \hat{U}_1^H, \qquad B_1 + B_2 = \hat{U}_2 \hat{D}_2 \hat{U}_2^H;$$

Step 4. Construct the commutative quaternion unitary matrix U and the commutative quaternion upper triangular matrix D of A as follows,

$$U = \frac{\hat{U}_1 + \hat{U}_2}{2} + \frac{\hat{U}_2 - \hat{U}_1}{2}\mathrm{j}, \ D = \frac{\hat{D}_1 + \hat{D}_2}{2} + \frac{\hat{D}_2 - \hat{D}_1}{2}\mathrm{j}.$$

4 Color image watermarking based on SchurCQ

To enhance the robustness of color watermark embedding and extraction, we performed NSCT [21] on color host images. NSCT realizes fine decomposition of the image by a nonsubsampled pyramid and nonsubsampled directional filter, and the decomposed subimage has the same size as the original image. The sum of all subimages is equal to the original image with translation invariance, which can effectively prevent the Gibbs phenomenon. Fig.1a shows the original image and Fig.1b shows the low-frequency image after NSCT processing. From Fig.1, it can be seen that the low-frequency image of NSCT concentrates most of the energy of the original image. Therefore, embedding the color watermark information into the low-frequency image can improve the robustness.

To increase the security of watermark embedding and extraction, we perform Arnold scrambling [22] for color watermarks. Arnold scrambling is an image encryption technique based on the Arnold transform, which is

(a) (b)

Fig. 1. NSCT decomposition

commonly used to encrypt and scramble images. The core idea is to rearrange the pixel coordinates of an image by a discrete linear transformation, so that the image becomes scrambled. The formula of the Arnold transform is as follows:

$$\begin{pmatrix} x' \\ y' \end{pmatrix} = \begin{pmatrix} 1 & 1 \\ 1 & 2 \end{pmatrix} \begin{pmatrix} x \\ y \end{pmatrix} \mod N$$

where (x, y) denotes the position of the pixel in the original image, (x', y') denotes the new position of the pixel after the Arnold transform, and N is the size of the image (usually $N \times N$ for a square image). By repeatedly applying this transform, the image pixel positions are perturbed many times, and eventually, the image becomes unrecognizable. It is worth noting that this transformation is periodic and after a certain number of iterations, the image can be restored to its original state, as shown in Fig.2.

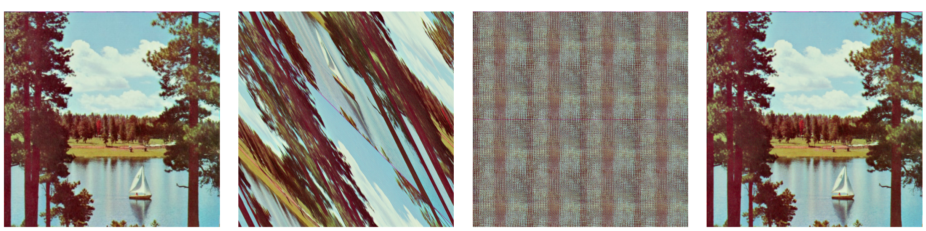

(a) original image 512×512 (b) scrambling times=1 (c) scrambling times=96 (d) scrambling times=384

Fig. 2. Arnold scrambling

The flowchart of color image watermark embedding and extraction based on SchurCQ is shown in Fig.3.

4.1. Color watermark embedding.

Step 1: Arnold scrambling is performed on the color watermark W, and then the scrambled decimal pixel values are converted to 8-bit binary numbers, which are concatenated into strings of 0 or 1 in turn. NSCT decomposition is performed on the host image A to extract the low-frequency image.

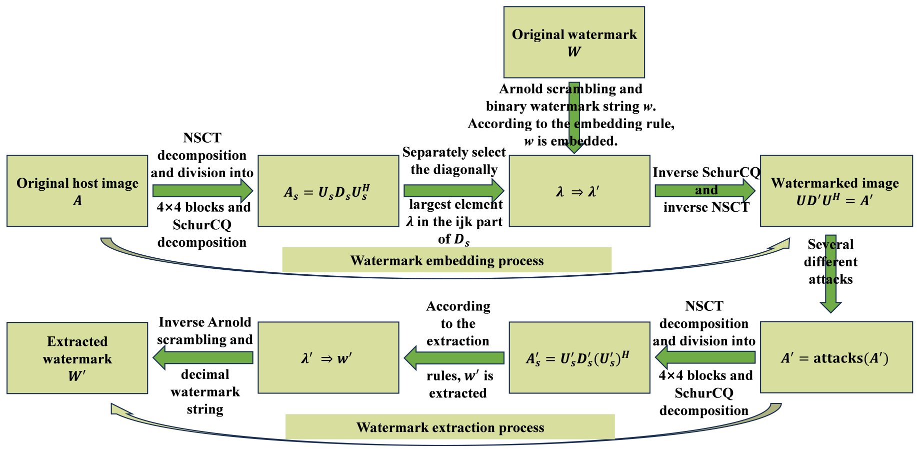

FIG. 3. Flowchart for color image watermark embedding and extraction

Step 2: using Algorithm 1, after dividing the low-frequency image into 4×4 non-overlapping blocks, perform SchurCQ decomposition to obtain $A_s = U_s D_s U_s^H$. Embed the 8-bit binary numbers w of the color watermark onto the largest diagonal element $\lambda_{\mathrm{i/j/k}}$ of the three imaginary parts $\mathrm{i}, \mathrm{j}, \mathrm{k}$ of D_s according to the following rules.

$$\begin{cases} \text{if } \mathrm{xor}(\mathrm{mod}(\mathrm{round}(\lambda_{\mathrm{i/j/k}}/QT), 2), w) == 0 \\ \qquad \lambda'_{\mathrm{i/j/k}} = \mathrm{round}(\lambda_{\mathrm{i/j/k}}/QT) \times QT + 0.5 \times QT; \\ \text{else} \\ \qquad \lambda'_{\mathrm{i/j/k}} = \mathrm{round}(\lambda_{\mathrm{i/j/k}}/QT) \times QT - 0.5 \times QT, \end{cases} \tag{13}$$

where QT: the given quantization step, round(x): rounds x to the nearest integer, mod(a, b): calculates the remainder of a divided by b, and xor(a, b): returns the XOR result of a and b, i.e., returns 1 when a and b are different, and 0 when they are the same.

Step 4: Use the new $\lambda'_{\mathrm{i/j/k}}$ to replace $\lambda_{\mathrm{i/j/k}}$ to obtain the new D'_s, and then use the inverse SchurCQ decomposition to obtain the watermarked image A'_s.

$$U_s D'_s U_s^H = A'_s.$$

When all elements in w have been used, we obtain the low-frequency watermarked image. By performing NSCT inverse operation on the low-frequency watermarked image, the complete watermarked image A' can be obtained. It should be noted that the commutative quaternion matrix A' generated by the algorithm is still close to the pure imaginary commutative quaternion matrix, that is, the real part of A' is close to zero.

4.2. Color watermark extraction.
Step 1: Use NSCT decomposition to extract a low-frequency image from the watermarked image.

Step 2: Using Algorithm 1, after dividing the low-frequency image into 4×4 non-overlapping blocks, SchurCQ decomposition is performed to obtain $A'_s = U'_s D'_s (U'_s)^H$. The 8-bit binary numbers w' of the color watermark are extracted from the largest diagonal element $\lambda'_{\mathrm{i/j/k}}$ of the three imaginary parts $\mathrm{i}, \mathrm{j}, \mathrm{k}$ of D'_s according to the following rules.

$$\begin{cases} \text{if mod(fix}(\lambda'_{\mathrm{i/j/k}}/QT), 2) == 0 \\ \qquad w' = 0; \\ \text{else if mod(fix}(\lambda'_{\mathrm{i/j/k}}/QT), 2) == 1 \\ \qquad w' = 1, \end{cases} \tag{14}$$

where fix(x) rounds x towards zero to the nearest integer.

Step 3: Convert w' to a decimal vector and reorganize it into a matrix of the size of the color watermark. Next, inverse Arnold scrambling is performed to obtain W'.

5 Numerical experimenters

In order to better evaluate the effectiveness of color image watermark embedding and extraction, we need to introduce the evaluation metrics Peak Signal-to-Noise Ratio (PSNR) and Normalized Crosscorrelation (NC).

PSNR is an important metric to measure the quality of an image. PSNR evaluates the degree of distortion in an image by calculating the ratio of the maximum pixel value to the Mean Squared Error (MSE) between the original image and the processed image. It is defined by the formula:

$$\mathrm{PSNR} = 10 \times \log_{10} \left(\frac{3n^2 \times \mathrm{MAX}^2}{\sum_{x=1}^{n} \sum_{y=1}^{n} \sum_{z=1}^{3} (A(x,y,z) - \hat{A}(x,y,z))^2} \right),$$

where MAX is the maximum possible value of an image pixel (e.g., for an 8-bit image, MAX = 255), $A(x, y, z)$ is the pixel value of the original image at pixel position (x, y, z), $\hat{A}(x, y, z))$ is the pixel value of the processed image at pixel position (x, y, z), and n is the size of the image.

NC is used to evaluate the similarity between the extracted watermark and the original watermark. It is defined by the formula:

$$\mathrm{NC} = \frac{\sum_{x=1}^{m} \sum_{y=1}^{n} \sum_{k=1}^{3} W(x,y,z) \times \hat{W}(x,y,z)}{\sqrt{\sum_{x=1}^{m} \sum_{y=1}^{n} \sum_{z=1}^{3} W(x,y,z)^2} \sqrt{\sum_{x=1}^{m} \sum_{y=1}^{n} \sum_{z=1}^{3} \hat{W}(x,y,z)^2}},$$

where $W(x, y, z)$ and $\hat{W}(x, y, z)$ denote the pixel values of the original watermark and the extracted watermark at pixel location (x, y, z).

5.1. Dataset and quantization step.

We use four color images of 512×512 size from USC-SIPI [23] as color host images as shown in Fig.4. Fig.5 shows two color watermarks of 32×32 size.

(a) Baboon (b) Airplane (c) Boat (d) House

FIG. 4. Color host images

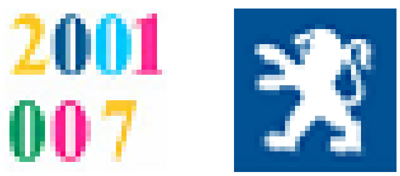

(a) (b)

FIG. 5. Color watermarks

Since the quantization step QT is a critical factor influencing the overall performance of the proposed scheme, we conducted a detailed analysis of its impact. Initially, Fig.5a and Fig.5b were embedded into Fig.4a-d respectively, with the quantization step ranging from 2 to 40, in increments of 2. The PSNR values between the watermarked images and the host images were calculated, along with the NC values between the extracted watermarks and the original watermarks.

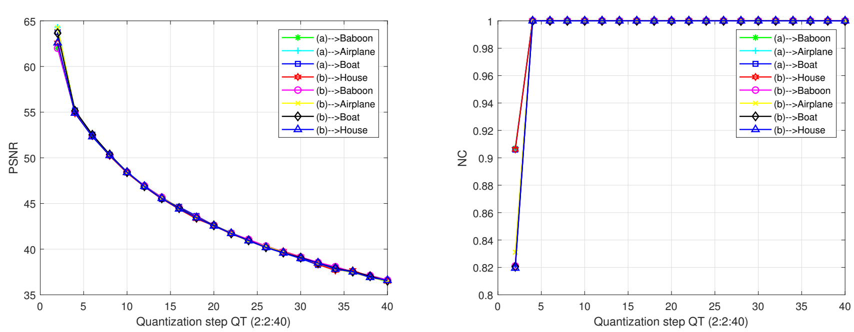

FIG. 6. PSNR and NC values for different quantization steps

Fig.6 illustrates the corresponding trends in PSNR and NC values. It can be observed that as the quantization step increases, the PSNR values gradually decrease, while the NC values gradually tend to 1. This indicates that with the increase in the quantization step, the imperceptibility of the watermarking algorithm diminishes, whereas its robustness is enhanced. Therefore, the optimal quantization step can be dynamically selected according to the specific requirements for imperceptibility and robustness in different scenarios. Fig.7 shows the extracted watermarks and the watermarked image when the quantization step QT is 26.

FIG. 7. PSNR values of different watermarked images and NC values of extracted watermarks

5.2. Robustness test and analysis.

In addition to the aspects we have previously discussed, the robustness of a watermarking algorithm is also crucial, specifically its ability to withstand various attacks. High robustness is a key factor in a good watermarking scheme, primarily reflected in the capability to extract the complete watermark from the attacked watermarked image. Next, we study the performance of the watermarking scheme when it is attacked by JPEG2000, salt & pepper noise, Gaussian noise, blurring, Gaussian low pass filtering, Gaussian smooth filtering, and Poisson noise. In this experiment, the quantization step QT is 40, and the parameters of the compared schemes [14] and [16] are 0.25 and 26 respectively. In this experiment, the host image is the "House" in Fig.4, and the watermark is Fig.5a. Using these schemes, the NC values between the extracted watermark and the original watermark are shown in Tab.1.

Attack	Proposed scheme	Scheme [16]	Scheme [14]
JPEG2000 (4:1)	1.0000	1.0000	0.9756
JPEG2000 (7:1)	1.0000	0.9994	0.8695
Salt & pepper noise (5%)	0.9058	0.8982	0.8960
Salt & pepper noise (1%)	0.9784	0.9747	0.9674
Gaussian noise (0, 0.003)	0.9677	0.9063	0.9665
Gaussian noise (0, 0.001)	0.9961	0.9759	0.9847
Blurring ([5,5], 0.5)	0.9955	0.9911	0.9932
Gaussian low pass filtering (250)	0.9996	0.9954	0.9942
Gaussian smooth filtering (150)	0.9926	0.9854	0.9669
Poisson noise	0.9801	0.9372	0.9727

Table 1. Comparison of robustness under different attacks.

Based on Tab.1, the proposed scheme demonstrates superior robustness under most attack conditions, particularly in the cases of JPEG2000 compression (4:1 and 7:1), Gaussian noise (0,0.001), blurring ([5,5],0.5), Gaussian low pass filtering, Gaussian smooth filtering and Poisson noise, where the scheme achieves performance metrics close to or equal to 1, outperforming scheme [14] and scheme [16]. However, under the attack of salt and pepper noise (5%), the robustness of the proposed scheme is slightly worse. Nevertheless, the proposed scheme demonstrates more stable and superior robustness across various attacks, particularly excelling in handling compression, blurring, and noise attacks.

6 Conclusions

In this paper, we proposed a novel color image watermarking scheme that integrates the nonsubsampled contourlet transform with the Schur decomposition of commutative quaternion matrices. The proposed method effectively embeds watermark information into the low-frequency components of the host image, significantly improving the robustness and security of the watermark against various attacks. The use of Arnold scrambling further enhances the security by ensuring the unpredictability of the watermark's location. Numerical experiments demonstrate that our scheme outperforms schemes [14, 16] in imperceptibility and robustness, as evidenced by high NC values between the original and extracted watermarks. The paper provides a reliable and efficient scheme for copyright protection in digital image processing, with applications for securing multimedia content in today's interconnected world. Future work may explore the extension of this approach to other types of multimedia data and the application of advanced machine-learning techniques to further enhance the robustness of the watermarking process.

References

[1] G. Hua, J.W. Huang, Y.Q. Shi, J. Goh, V.L.L. Thing, *Twenty years of digital audio watermarking—a comprehensive review*, Signal Processing, **128** (2016), 222-242.

[2] C. Qin, P. Ji, X.P. Zhang, J. Ding, J.W. Wang, *Fragile image watermarking with pixel-wise recovery based on overlapping embedding strategy*, Signal Processing, **138** (2017), 280-293.

[3] M. Begum, M.S. Uddin, *Digital Image Watermarking Techniques: A Review*, Journal of Applied Mathematics, **11**:2 (2020), 110.

[4] Y. Li, M.S. Wei, F.X. Zhang, J.L. Zhao, *A New Double Color Image Watermarking Algorithm Based on the SVD and Arnold Scrambling*, Journal of Applied Mathematics, **2016** (2016), 1–9.

[5] S.C. Pei, J.H. Chang, J.J. Ding, *Commutative reduced biquaternions and their Fourier transform for signal and image processing applications*, IEEE Transactions on Signal Processing, **52**:7 (2004), 2012 –2031.

[6] T.S. Jiang, Z.W. Guo, D. Zhang, V.I. Vasil'ev, *A fast algorithm for the Schrodinger equation in quaternionic quantum mechanics*, Applied Mathematics Letters, **150** (2024), 108975.

[7] D. Zhang, T.S. Jiang, C. Jiang, G. Wang, *A complex structure-preserving algorithm for computing the singular value decomposition of a quaternion matrix and its applications*, Numerical Algorithms, **95** (2024), 267–283.

[8] D. Zhang, T.S. Jiang, Z.W. Guo, V.I. Vasil'ev, *Real and complex solutions of the total least squares problem in commutative quaternionic theory*, Computational and Applied Mathematics, **43** (2024), 235.

[9] D. Zhang, T.S. Jiang, Z.W. Guo, V.I. Vasil'ev, *An efficient method for the total least squares problem in reduced biquaternionic electromagnetics*, Computational and Applied Mathematics, **138** (2023), 826.

[10] D. Zhang, T.S. Jiang, G. Wang, V.I. Vasil'ev, *Two novel numerical methods for the diagonalisation of a reduced biquaternion matrix in the reduced biquaternionic algebra*, Computational and Applied Mathematics, **72**:1 (2022), 139-152.

[11] D. Zhang, G. Wang, V. I. Vasil'ev, T.S. Jiang. *Algebraic methods for equality constrained least squares problems in commutative quaternionic theory*, Mathematical Methods in the Applied Sciences, **46**:2 (2022), 1699-1708.

[12] P. Bas, N.L. Bihan, J.M. Chassery, *Color image watermarking using quaternion Fourier transform*, 2003 IEEE International Conference on Acoustics, Speech, and Signal Processing, **3** (2003), III-521.

[13] Y. Chen, Z.G.Jia, Y. Peng, Y.X. Peng, D. Zhang, *A new structure-preserving quaternion QR decomposition method for color image blind watermarking*, IEEE Transactions on Signal Processing, **185**:7 (20021), 108088.

[14] M.C. Zhang, W.X. Ding, Y. Li, J.H. Sun, Z.H. Liu, *Color image watermarking based on a fast structure-preserving algorithm of quaternion singular value decomposition*, Signal Processing, **208** (2023), 108971.

[15] D. Zhang, T.S. Jiang, G. Wang, V.I. Vasil'ev, *On singular value decomposition and generalized inverse of a commutative quaternion matrix and applications*, Applied Mathematics and Computation, **460** (2024), 128291.

[16] F.X. Hu, H.J. Cao, S.Y. Chen, Y.H. Sun, Q.T. Su, *A robust and secure blind color image watermarking scheme based on contourlet transform and Schur decomposition*, Visual Computer, **39** (2023), 4573—4592.

[17] Q.T. Su, Y.G. Niu, X.X. Liu, Y. Zhu, *Embedding color watermarks in color images based on Schur decomposition*, Optics Communications, **285**:7 (2012), 1792–1802.

[18] J.Z. Li, C.Y. Yu, B.B. Gupta, X.C. Ren, *Color image watermarking scheme based on quaternion Hadamard transform and Schur decomposition*, Multimedia Tools and Applications, **77** (2018), 4545-4561.

[19] C. Segre, *The real representations of complex elements and extension to bicomplex systems*, Mathematische Annalen , **40** (1892), 413-467.

[20] G.H. Golub, C.F. Van Loan, *Matrix computations. 4th Edition*, Johns Hopkins University press, Baltimore, 2013.

[21] A.L. Da Cunha, J. Zhou, M.N. Do, *The Nonsubsampled Contourlet Transform: Theory, Design, and Applications*, IEEE Transactions on Image Processing, **15**:10 (2006), 3089 – 3101.

[22] V.I. Arnold, A. Avez, *Ergodic problems of classical mechanics*, Addison-Wesley, Benjamin, 1968.

[23] University of Southern California, *Signal and Inage Processing Institute: USC-SIPI Image Database*, 1997.

Dong Zhang
North-Eastern Federal University,
NEFU, Belinsky St., 58,
677000, Yakutsk, Russia
Email address: dz_zhangdong@sina.com